Composite Ion Exchange Membrane Based Electrodialysis Cell For Desalination as well as Acid and Alkali Productions

[1]Krishnaveni Venugopal and [2]Sangeetha Dharmalingam
[1]Research Scholar, [2]Assistant Professor
[1,2]Department of Mechanical Engineering, Anna University, Guindy, Chennai, Tamil Nadu, India

Abstract — The various desalination process parameters for the fabricated bipolar membrane electrodialysis unit were investigated in this paper by using functionalized polysulfone based monopolar and bipolar type of ion exchange membranes. In the case of bipolar membrane, platinum was used as the intermediate layer. The synthesized membranes were characterized using FTIR, SEM and TGA to evaluate them structurally, morphologically and thermally. A commercially procured ion exchange membrane made of polystyrene divinyl benzene was also evaluated for the purpose of comparison. The electrodialysis process using these ion exchange membranes reached a highest current efficiency of 68.6 % and 38 % with the energy consumption of 0.50 Wh and 1.60 Wh for the synthesized and commercial membrane respectively.

Keywords— Electrodialysis; Brine Solution; Desalination; SEM; Membrane stack unit.

I. INTRODUCTION

To date, the desalination of seawater and of brackish water has been considered as a technical solution for the domestic, agricultural and industrial water demand. This is because when the demand increases the cost of developing new sources or expanding existing ones is getting higher as most accessible water resources like surface water, lakes, rivers and groundwater have largely been tapped. From both an economic and environmental point of view, saving or treating the available water rather than developing new sources is often the best 'next' source of water. And hence, the attentions of the researchers are gone towards improving the water treatment processes with reduced costs.

Membrane processes are found to have considerable advantages in desalting brackish water and are being widely applied in the market. A multi-compartment ED apparatus [1] consisting of two electrodes and a stack of ion exchange membranes (IEMs) between them is one among membrane technology that has some advantages over reverse osmosis [2] in the treatment of certain brackish waters [3] and for acid-base recovery during salt desalination under specific environments. The efficiency of the ED process strongly depends on the type of IEM chosen for the process and it can be monopolar and bipolar in nature depended on its application purpose. The importance of bipolar membrane (BPM) is its water splitting capability during ED [4]. The water dissociation noticed in a conventional ED process decreases current efficiency (CE) and gives rise to scale troubles. Whereas the same attracts attention in a bipolar membrane electrodialysis (BPMED) process because it increases CE. BPMED process is a combination of conventional ED and water dissociation feature due to the presence of catalytic intermediate layer (IL) in BPM that allows the production of acid and base from their corresponding salt solutions.

The presence of heterogeneous materials like ion-exchange resin (IER) particles in a non-conducting polymer matrix layers of a BPM [5] and presence of catalytic intermediates like quaternary, non- quaternary amine group, weak acid and its corresponding base, inorganic substances, metallic compounds, heavy/noble metal ions, macromolecules, dendrimers etc. [6-8] in between the cation exchange layer (CEL) and anion exchange layer (AEL) as IL usually results in BPM with higher mechanical stability [9,10] with improved water dissociation effects when compared with the BPM prepared with laminating CEL and AEL alone without any IL.

In the present work, monopolar (cation exchange (CEM) and anion exchange (AEM)) and bipolar (with platinum (Pt) as IL) IEMs with resin and glass fiber reinforcements were prepared using polysulfone (PSu) polymer. The prepared IEMs were characterized using FTIR, SEM, TGA, contact angle and some laboratory techniques. Water dissociation capacity of the prepared BPM with Pt intermediate was tested in a two compartment electrodialytic cell. The membranes were evaluated for their desalination efficiency on diluted real sample brine solution of approximately 10,000 ppm up to 8 h. The stack performance using the synthesized membranes was compared with that of the commercial polystyrene divinylbenzene based (PSDVB) ion exchange membranes under similar experimental conditions. In addition, the decrease in sodium-chloride ion concentration, salinity and electrical conductivity of the feed water were observed.

II. EXPERIMENTAL METHODOLOGY

A. Required Materials

Commercial strong acid cation exchange membrane (CMI – 7000S) and commercial strong base anion exchange membrane (AMI – 7001S) were procured from Membranes International INC, New Jersey, USA. While, BPM made up of PSDVB were procured from Arun Electro chemicals, Chennai. Glass fiber was purchased from Meena glass fiber industry. Seralite (Cation Exchange resin (CER) - equivalent to Amberlite IRC - 120, 20-50 mesh standard grade) and Seralite (Anionic exchange resin (AER) - equivalent to Amberlite IRA - 400, 20-50 mesh standard grade) were obtained from Sisco Research Laboratory Pvt. Ltd. (SRL). Platinum chloride (Pt) and Polysulfone (PSu) [Mn=16,000 (MO), Mw=35,000 (LS)] was purchased from Aldrich (USA).

B. Preparation of Reinforced IEMs

Anionic and cationic functionalized ionomer membranes of sulfonated polysulfone (SPSu) and quaternized polysulfone (QPSu) was carried out as per the procedure reported earlier [11]. To enhance additional functions like higher ion exchange capacity (IEC), firmness and strength of the membranes, its surface was modified using resin and glass fiber. Reinforced cationic and anionic exchange membrane (RCEM & RAEM) based on functionalized PSu polymer was prepared by first

dispersing a specific quantity (from 10 % to 70 %) of dried (60 °C for 24 h in an oven) and crushed cationic/anionic exchange resin (CER/AER) in SPSu/QPSu - N, N′- dimethyl formamide (DMF) solution for 12 h using a magnetic stirrer at room temperature. In order to break the aggregates and to obtain a uniform dispersion, the solution was sonicated for 30 min. Then, the solution was cast on a clean glass petridish and the glass fiber matrix was placed to get immersed in the solution before drying in the oven for 24 hours at 80 °C. The conductivity of the prepared membranes increased with increase in IER loadings up to 50 % beyond which the membranes became brittle (Table 1). Hence, the resin loading was optimized at 40 % for both resins [12]. Reinforced bipolar membrane (RBPM i.e. RPSu-Pt) was prepared using RCEM (RSPSu) and RAEM (RQPSu) as CEL and AEL respectively. Then on one side of both CEL and AEL layers, a solution containing approximately 6 mL of 0.12 g of Pt contained solution was coated to form the IL. Finally the IL coated side of both layers (CEL and AEL) were sandwiched and subjected to hot press to finally obtain RBPM represented as RBPM-Pt.

C. Characterization of Reinforced IEMs

The incorporation of resin into functionalized PSu membrane was confirmed with Perkin Elmer RX I FTIR spectrophotometer. The thermal stability of the prepared membranes were studied using SDT Q 600 US analyzer (ASTM E1131) under nitrogen atmosphere with a heating rate of 20 ℃/minute from room temperature to 700 °C. The morphology of the membranes was studied using field emission HITACHI S-3400 SEM instrument. The hydrophilic and hydrophobic nature of the membranes was determined using Goniometer-sessile drop meter GBX–Digi-drop wetting and spreading studies. The conductivity of the membranes was determined using impedance spectroscopy. Water absorption and IEC for the prepared membranes were measured as discussed earlier [11]. The chemical stability of membranes was analyzed by accelerating the degradation process using a solution containing 4 ppm of ammonium iron (II) sulfate hexahydrate and 15 mL of H_2O_2 (3 %) (Fenton's reagent) in 500 mL distilled water at 60 °C for about an hour.

Table 1: Optimization Of Resin Loadings In Psu Polymer Using Its Conductivity

% of resin added	CER Conductivity (S/cm)	AER Conductivity (S/cm)
10	1.68×10^{-6}	8.69×10^{-7}
20	2.78×10^{-6}	4.78×10^{-6}
30	5.31×10^{-6}	7.57×10^{-6}
40	4.76×10^{-5}	3.8×10^{-5}
50	3×10^{-5}	2.73×10^{-5}
60	2.39×10^{-6}	1.79×10^{-6}
70	1.7×10^{-6}	1.2×10^{-6}

D. Design and Working of Multi-Compartment ED Stack

The 5 compartment BPMED unit (Fig. 1(b)) used in the study for the determination of IEM performance towards desalination was supplied by Arun Electrochemical, Chennai. The same instrument was altered into two compartments set up for the determination of BPM efficiency (Fig. 1(a)). The cathode and anode electrodes used were stainless steel and Ti coated with Ti-Ru-Pd oxides, respectively. The active

membrane area of each membrane and volume of each chamber was about 120 cm^2 and 160 cm^3 respectively. Each compartment was connected to a tank of 1 L capacity, allowing for batch wise recirculation mode operation of external solutions using submersible pumps. The configuration of the membrane arrangement in the multi compartment ED stack is BPM-AEM-CEM-BPM and the five compartments of the BPMED unit were EC-AC-FC-BC-EC (where, EC stands for electrolyte compartment placed at the two extremes, adjacent to the electrodes; FC stands for feed compartment; AC and BC stands for acid and base compartments respectively, placed adjacent to the feed compartment on either side) as represented in Fig. 1(b).

In order to minimize the cell voltage generated during the initial stages of the performance, dilute HCl (0.01 N) and dilute NaOH (0.01 N) solutions were used in AC and BC respectively. And 0.05 mol/L of NaCl solution was used in each EC. Because at lower concentrations, higher resistances between membranes resulted and at higher concentrations, the selectivity nature of the IEMs became lower. During the performance, at every 15 minutes time interval, process parameters such as membrane stack potential, conductivity, pH and acid-base concentration of the solutions in various compartments were determined. In addition, other parameters such as energy consumption, current efficiency (CE), Transport number (T. No.) of ions, water dissociation efficiency (WDE) and water dissociation flux were determined using the same set of equations as reported earlier [7,8]. Finally, after 8 hours of treatment, the feed sample was analyzed for their salinity and electrical conductivity using WTW LF 197-S EC meter. The concentrations of chloride and sodium ions of the samples were measured by argentometric method and flame photometry respectively.
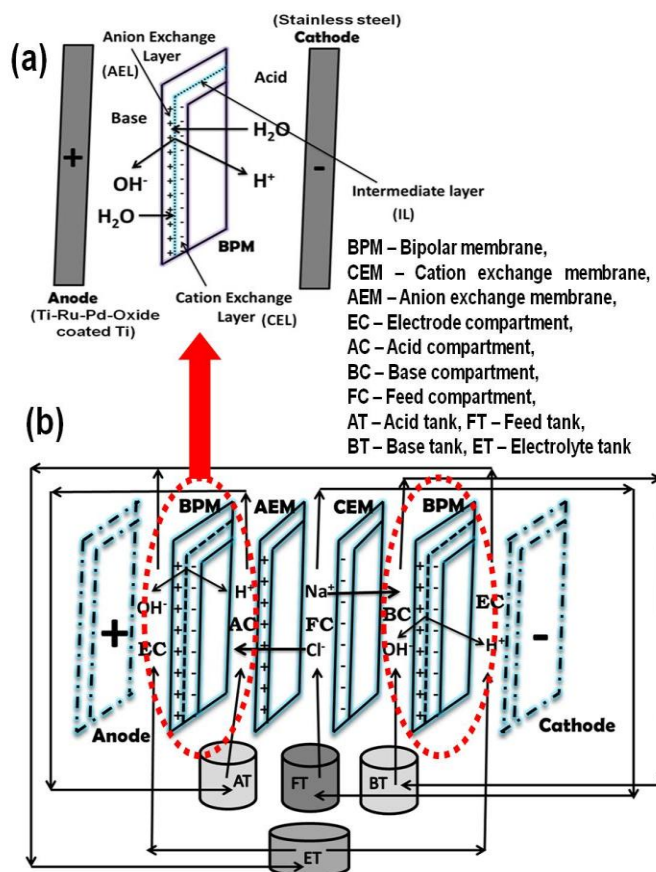

Fig. 1. Schematic representation of (a) Two compartment electrodialytic cell for BPM efficiency (b) Five compartment electrodialytic cell for brine desalination.

III. RESULTS AND DISCUSSION

A. FTIR Characterization

Pristine PSu, RCEM (RSPSu) and RAEM (RQPSu) membranes were characterized by FTIR (Fig. 2) to confirm their structure and the incorporation resin. The appearance of bands at 3026 cm^{-1} and 756 cm^{-1} in Fig. 2 (a) was due to the ν_s (C-H) and δ (C-H) vibration bond of aromatic hydrocarbons respectively. Appearance of bands at 1411 cm^{-1} and 1387 cm^{-1} was due to the aliphatic ν_{as} (C-H) and ν_s (C-H) vibration respectively. A doublet peak at 1589 cm^{-1} was due to Aromatic ν_s (C=C) vibration. The peaks at 1163 cm^{-1} and 1320 cm^{-1} were due to the ν_s (SO$_2$) & ν_{as} (SO$_2$) group vibration respectively. The peak at 692 cm^{-1} was due to ν (C-S) vibration and peak at 1113 cm^{-1} and 1298 cm^{-1} represents ν_s (C-O-C) & ν_{as} (C-O-C) vibrations respectively. The appearance of all these peaks confirmed the structure of PSu. The appearance of a broad and more intense envelope around 3447 cm^{-1} in Fig. 2(b) due to –OH stretch of sulfonic acid group (present in both resin and membrane matrix) and peak around 1161 cm^{-1} due to the O=S=O (asymmetric stretch) confirmed the sulfonated form of PSu in RSPSu membrane. The appearance of a peak at around 854 cm^{-1} showed that sulfonic acid group was substituted at para position. The broad peak at 3392 cm^{-1} in Fig. 2(c) was assigned to the characteristic peak of ν_{as} (NR$_3^+$). The appearance of peak around 1320 cm^{-1} due to C-N stretching vibration confirmed the amine group in the RQPSu membrane matrix.
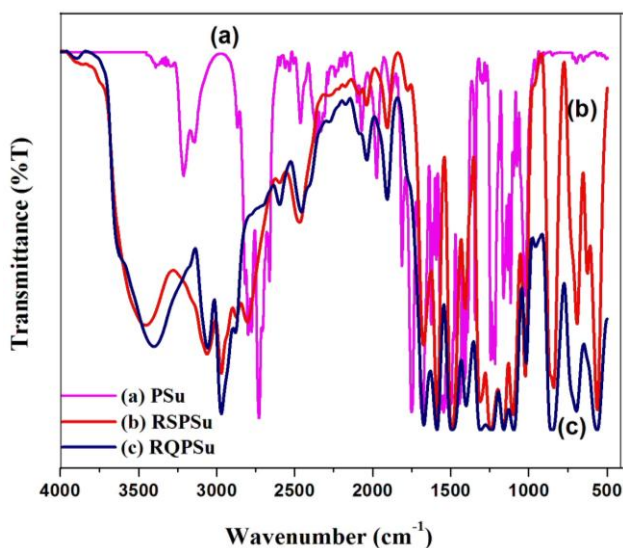

Fig. 2: FTIR spectra of (a) PSu, (b) RSPSu and (c) RQPSu membranes

B. Thermo Gravimetric Analysis

The TGA curves of the reinforced monopolar and bipolar membranes are shown in Fig. 3. The reason for the various degradation steps observed at certain temperatures are represented in Table 2. The TGA curve of pristine PSu, as observed in Fig. 3 (a), exhibited two stages of degradation. The first step indicated the loss of bound water and traces of solvent up to 270 °C beyond which no further weight loss was observed until 476 °C. The steep loss in weight observed beyond 490 °C suggested polymer degradation.

Table 2: Degradation temperatures and their reasons for various IEMs

Reason for degradation	RSPSu (3 steps as from Fig. 3 (b))	RQPSu (3 steps as from Fig. 3 (c))	RBPM-Pt (4 steps as from Fig. 3 (d))	BPM-PSDVB (3 steps as from Fig. 3 (e))
Removal of water and solvent traces that was physically adsorbed and chemically bonded from the polymer matrix	up to 152 °C	up to 137 °C	up to 143 °C	up to 129 °C
Degradation of functional groups (sulfonic acid group and / or quaternary ammonium group) from the polymer chain	366 °C – 438 °C (SO$_3$H)	266 °C – 404 °C (-NR$_3^+$)	325 °C – 357 °C (both)	249 °C – 311 °C (both)
Removal of loosely bound IER particles present on the surface and from the polymer matrix			345 °C – 392 °C	--
Degradation of intermediate molecules	--	--		
Removal of reinforced fiber from the polymer matrix	504 °C – 578 °C	beyond 529 °C	beyond 430 °C	beyond 336 °C
Polymer main chain degradation				

C. SEM Analysis

The morphology of various IEMs such as RSPSu, RQPSu and RPSu-BPM are shown in Fig. 4. A uniform distribution of resin particles throughout the reinforced membrane surface was observed in the surface SEM images of RSPSu and RQPSu membranes. On the other hand, cross sectional view of reinforced PSu-Pt based BPM i.e. RPSu-BPM clearly showed three distinct regions. The top layer was anion exchange layer (AEL) or RQPSu while the thin middle one represented the Pt – IL and the third layer correspond to the cation exchange layer (CEL) or RSPSu. The appearance of small spheres on both top and bottom surfaces of RPSu-BPM shows the presence of IER particles.
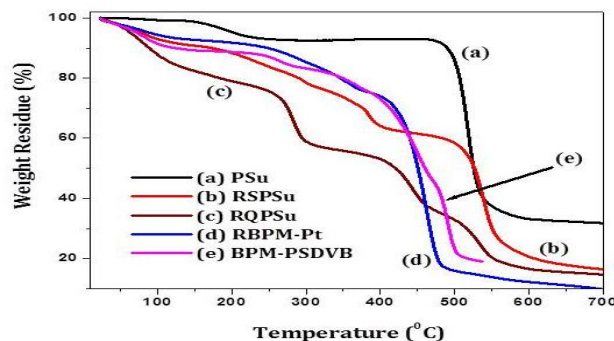

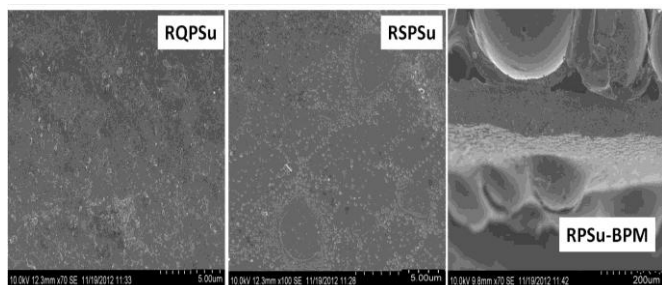Fig. 3: TGA curves of (a) PSu, (b) RSPSu, (c) RQPSu, (d) RBPM-Pt and (e) BPM-PSDVB

Fig. 4: SEM images of surface views of RSPSu and RQPSu membranes; and cross sectional view of RPSu-BPM membrane

D. Contact Angle Measurement

From Fig. 5, it was identified that the introduction of functional group converts the hydrophobic polymer (82.51°) into hydrophilic polymer with a smaller contact angle as studied by Dias & de Pinho [13] and Guan et al [14]. The contact angles of the commercial monopolar membranes such as CEM-PSDVB and AEM-PSDVB were measured to be 86.70° and 93.09° respectively. Contact angle value for the reinforced functionalized membranes such as RSPSu and RQPSu could not be measured due to complete absorption of water. This infers that the increased hydrophilicity of these membranes than the pristine membrane was due to the presence of functional groups, resins and fiber reinforcements [15]. In order to determine the nature of Pt intermediate in BPM, one face of the membrane was coated with Pt solution and its contact angle was measured and was found to be 54.88°.

E. Chemical stability

To determine the suitability of the prepared reinforced IEMs and commercial IEMs in BPMED unit, all the membranes were subjected to chemical stability test using Fenton's reagent. The generated peroxides attacked the polymer chains to undergo faster degradation. All the subjected samples were then checked for their water absorption, IEC and conductivity values as per the standard procedures [11] and the values are tabulated in Table 3. Although the reinforced fibers held the IEMs strongly, due to enhanced degrading mechanism, the incorporated hydrophilic resins and functional groups that were present on the surface leached out from the membranes due to loosening of the fibers upon swelling which resulted in lower IEC, water absorption and conductivity values [16].

Fig. 5: Contact angles of water droplets on various membrane surfaces

Table 3: Chemical stability test

Membrane Code	IEC (meq/g)		Water absorption (%)		Conductivity (10^{-3} S cm^{-1})	
	Initial	Final	Initial	Final	Initial	Final
RSPSu	4.75	4.53	15.4	14.3	5.86	5.19
RQPSu	4.35	4.12	11.0	9.9	5.28	4.86
RBPM-Pt	-------		20	18.6	6.6	6.04
CEM-PSDVB	1.6	1.5	6.5	5.4	4.86	4.64
AEM-PSDVB	1.3	1.2	3.7	3.1	4.68	4.27
BPM-PSDVB	-------		9	8.2	4.75	4.4

F. Characterization of RPSu-Pt and PSDVB BPMs

(i) pH variation with time

Since BPM consisted of RCEM and RAEM as CEL and AEL layers respectively which were joined together using a catalytic Pt as IL, when it was placed in between the electrodes due to large electric field appearing at the membrane interface, an excess OH$^-$ and H$^+$ ions were produced by the enhanced chemical reaction. This then migrated through the ion exchange layers into the distilled water filled compartments resulting in the formation of acid and base. This acid and base yield was analyzed using change in pH measurements. From Fig. 6 it was obvious that with increase in time, pH of the solutions in the two compartments changed from its initial distilled water value. The compartment closer to the anode side was found to be basic in nature and the one closer to the cathode side was acidic in nature. The increasing trend in pH change with time confirmed that some ions were produced newly during the performance due to certain in-situ reactions. These ions probably were protons and hydroxyl ions and formed on either side of the BPM as a result of water splitting into its ions under the electrical driving force between the electrodes. This conclusion was arrived at ease as there was no possibility of any other ions formed since only distilled water was taken in both the compartments.
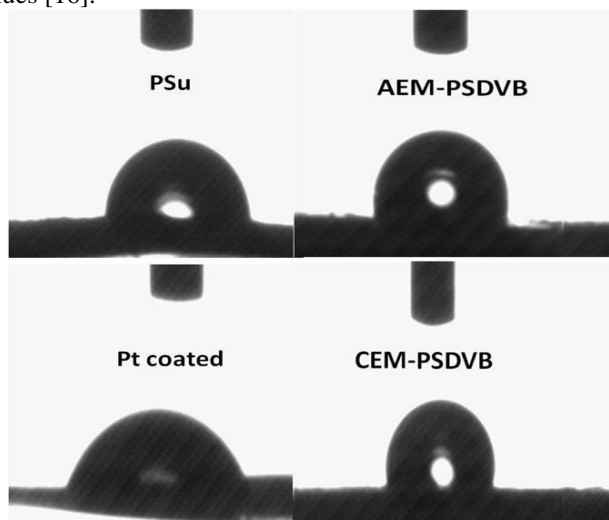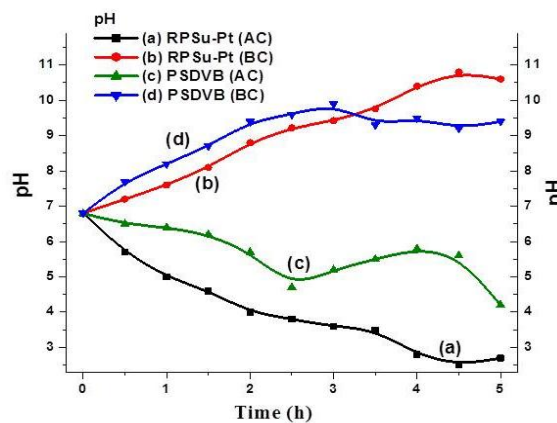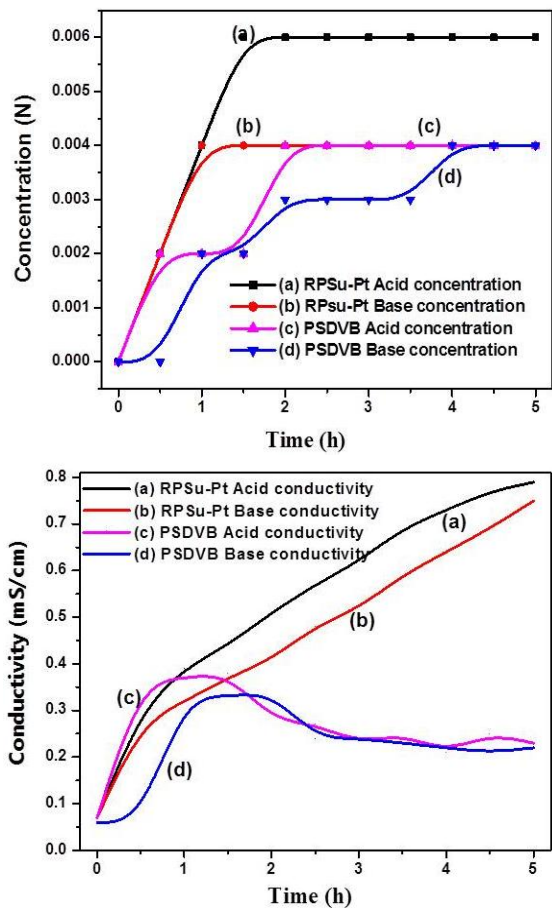
Fig. 6: pH, concentration and conductivity change with time in both AC and BC

(ii)   Concentration and conductivity changes with time

The conductivity meter was optimized before taking readings using the distilled water. Fig. 6 shows the change in conductivity of the acid and base solutions with time for both RPSu-Pt and commercial PSDVB BPMs. Initially, the acid conductivity rose from an initial value of 0.07 mS/cm to a maximum of 0.79 mS/cm and 0.38 mS/cm for both synthesized and commercial membranes respectively. Similarly, the base conductivity also rose from 0.07 mS/cm to a maximum of 0.75 mS/cm and 0.34 mS/cm for both synthesized and commercial membranes respectively. The sudden decrease in conductivity values after 2 h in case of PSDVB BPM was suggestive of greater leakage of ions via membranes to the neighboring compartments. Whereas in the case of RPSu-Pt BPM lower level of ion leakage was observed. However, between the two BPMs, PSDVB showed lower values of acidic and basic conductivities when compared to RPSu-Pt.

Additionally, the maximum concentration of 0.006 N and 0.004 N for both acid and base was achieved in about an hour in the case of RPSu-Pt when compared to PSDVB BPM (beyond 2 hours). In both BPMs, once higher concentration was reached in both AC and BC; decrease in concentration was observed for BPM which exhibited a higher leakage and was observed to get leveled off without further rise or decrease if the leakage was not much favored in BPM. Hence, from the above discussion and from Fig. 6, it was confirmed that RPSu-Pt showed a better performance than PSDVB.

(iii)   Current-Voltage relationship

Fig. 7 (a) and (b) represents the typical steady state I-V curves as reported [12]. It was clear from the figures that no

rectification was observed since current was measured under the applied voltage. The increase in current with increasing voltage proved the occurrence of water splitting in both the BPMs [17]. On comparing the potential applied during the performance of both BPMs, RPSu-Pt showed a higher value of up to 12.6 V than PSDVB (11 V) for the same duration; while the increase in current was observed to be slightly lower for RPSu-Pt (51 mA) than PSDVB (52 mA). In Fig. 7 (a) the variation in current due to ionic transportation was smaller when compared with Fig. 7 (b). This magnitude is a measure of BPM selectivity towards co-ion leakage, and used to predict its efficiency. Hence, it could be concluded that RPSu-Pt BPM was expected to have better process efficiency when compared to PSDVB BPM. Beyond this potential, water dissociation occurs and the water splitting products (OH^-/H^+) also participated in the current transport which resulted in a steep increase in current. From this region, it could be clearly understood that the onset of water dissociation reaction occurred earlier in the case of RPSu-Pt BPM than PSDVB BPM. The only reason for the better performance of the RPSu-Pt system was due to the presence of the Pt IL along with fiber and resin reinforcements in the case of RPSu-Pt when compared to the PSDVB system. On introduction of the IL and resin, the region between the ion exchange layers became hydrophilic and attracted more water to the space charge region resulting in lower resistance. Whereas, in the case of commercial BPM which was without catalyst, the water dissociation resistance increased with increase in current, due to slower water dissociation rate than the ion transfer rate. The above results confirmed that the introduced Pt intermediate in RPSu-Pt BPM functioned as an effective water dissociation catalyst.
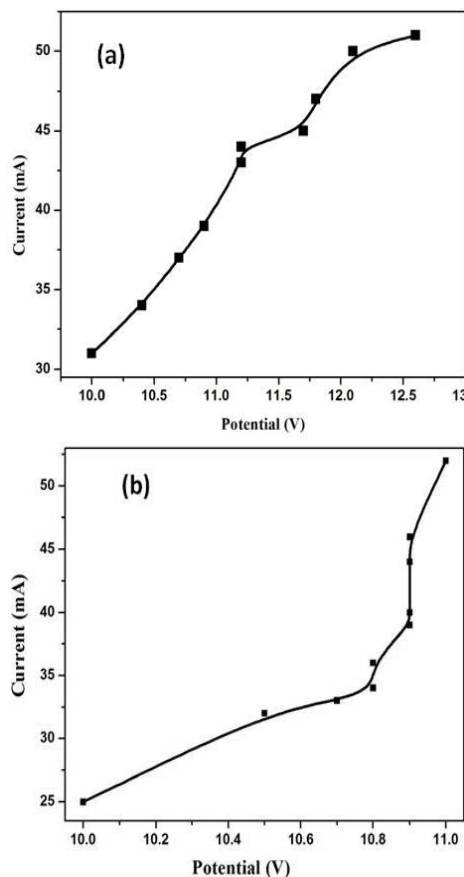

Fig. 7: Current-voltage curves for (a) RPSu-Pt and (b) PSDVB BPMs

G. BPMED stack performance for brine desalination

(i) Determination of pH and conductivity changes with time

Fig. 8 represents the pH and conductivity changes with time for both RSPSu-Pt and PSDVB systems. The pH of the solutions in FC, EC, AC and BC was observed regularly at every 15 min interval up to 8 h. In the case of RPSu-Pt system, the pH in FC was observed to increase towards basicity then decrease and finally become slightly acidic in nature which was similar to the results observed in literature [18]. This is because with increase in time, higher quantities of acid were produced due to water dissociated products and thereby resulting in proton leakage through IEMs depending upon the capacity of protons to undergo back diffusion. Due to its intrinsic mobility in the presence of water, FC remained slightly acidic in nature. On the other hand, in the case of PSDVB system, the feed solution finally became basic in nature. The difference in pH observed between the two different systems was mainly attributed to the leakage of ions occurring through the membranes between the compartments in a stack. PSDVB based cell experienced a greater leakage of ions from BC to FC and thus it remained basic in nature. It was also reported that the proton leakage through PSDVB IEM was lower due to lower concentrations of acid that was produced during BPMED process [18]. In the case of EC, due to the initial addition of 0.05M NaCl solution, the pH was observed to be slightly basic during the initial stages, which was then observed to be decreasing with time. Though both the IEM systems showed the final solution to be acidic, the acidity was greater in the case of PSDVB IEM system than that observed with RPSu-Pt IEM system. The reason for this was attributed to the higher leakage of ions through commercial membrane than the synthesized membrane.

From Fig. 8, it was clear that the initial pH in AC and BC was found to be in the range of ~ 2.45 and ~ 10.74 respectively due to the addition of 0.01N acid and 0.01 N base solutions into their respective compartments. Moreover, the pH in both AC and BC was found to rise marginally during the initial stage and was not uniform because of the leakage of certain ions into the neighboring compartments. Later, due to higher acid production, higher acidic pH and hence greater acid leakage was observed in case of RPSu-Pt IEM system when compared to PSDVB IEM system. Whereas, in the case of basic pH, both the systems showed more or less the same pH during the initial period of performance and later RPSu-Pt IEM system showed a little lower basic pH when compared to PSDVB IEM system. Such a pH change in AC and BC confirmed the acid-base production in their respective compartments which can also be confirmed by their conductivity and concentration measurements. This pH variation in various compartments clearly suggested that both systems possessed adequate capacity to split water into its co-ions under electric field.

Similar to the pH observations, in the case of conductivity too, AC and BC showed some initial conductivity. Since the ionic mobility of protons was higher than that of hydroxyl ions, the conductivity was found to be higher in the case of AC when compared to BC. The initial decrease in FC conductivity from 2.1 mS/cm to 1.2 mS/cm and 1.8 mS/cm was finally increased to 1.84 mS/cm and 3.0 mS/cm for RPSu-Pt and PSDVB respectively. In the case of AC, the increase in acidic conductivity reached a maximum (from an initial 0.5 mS/cm) of 1.25 mS/cm and 1.18 mS/cm for RPSu-Pt and PSDVB systems respectively. Similarly for BC, the basic conductivity increased from 0.10 mS/cm to a maximum of 0.77 mS/cm and 0.66 mS/cm for RPSu-Pt and PSDVB systems respectively. After reaching the maximum in both AC and BC, the conductivity slightly decreased or increased due to the loss of ions from this compartment or transfer of other ions from the neighboring compartment. Hence, the higher conductivity value was mainly due to the co-ions of water rather than the salt ions. This not only clearly confirmed the membrane's capacity to migrate ions from FC to the opposite electrodes but also proved the BPM's water dissociation capacity under electric field.
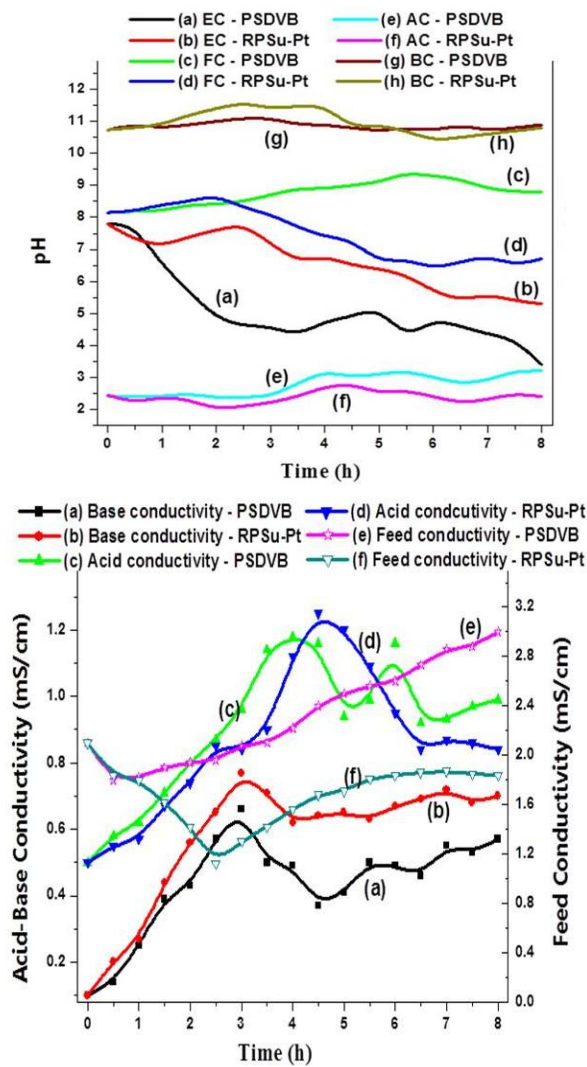

Fig. 8: Change in pH and conductivity in various compartments with time

(ii) Determination of acid-base concentration and current-voltage measurement

When the entire ED cell was under an electric field, the Na^+ and Cl^- ions were continuously transported from FC into BC and AC respectively. In addition to this, an excess OH^- and H^+ ions produced at the AEL-CEL interface due to the field enhanced chemical reaction also permeated through the IELs resulting in the acid-base formation. From the pH and conductivity studies, it was evident that acid and base of certain concentrations were produced in the AC and BC respectively for both the systems. From Fig. 9, it was noted that a maximum acid concentration of 0.014 N and 0.008 N was achieved for RPSu-Pt and PSDVB systems respectively.

Similarly, a maximum base concentration of 0.006 N and 0.004 N was achieved for RPSu-Pt and PSDVB systems respectively.

The commercial PSDVB IEM cell was meant for base production rather than acid production because of higher specific permselectivity of CEM for H^+ ions as reported in the literature [18]. However, in our study, from Fig. 9, the alkalinity concentration was observed to be lower in case of PSDVB system. This can be due to the higher intrinsic mobility of H^+ ions than the OH^- ions and hence resulting in higher leakage of H^+ ions. The T. No. of protons through AEM increased with acid concentration which would also lead to their lower concentration in AC. The maximum concentration remained constant until certain duration of time after which it decreased with increase in process time for both types of IEM system. This suggested that the mass transfer of Na^+ and Cl^- ions through the IEM diminished due to the decrease in NaCl concentration in the feed solution. Together with the increase in the concentration of Na^+ and Cl^- ions in BC and AC, the molecular back diffusion through IEM which was caused by the high concentration gradient might also hinder the transport of Na^+ and Cl^- ions. Furthermore, the dissociation of water molecules was also enhanced due to the Second Wien effect.

dissociation into hydrogen and hydroxyl ions, which causes the voltage across the membrane to fall. On the other hand, due to its catalytic activity, the increased use of Pt as an intermediate in turn increases the efficiency of water splitting.

(iii) Determination of WDE and T. No. of ions

The BPMED process efficiency is strongly affected by the transport properties of ions present in the solution and WDE. Under an electric field, at the beginning of the BPMED process, there was a competition between the ions such as Na^+, Cl^-, H^+ and OH^- for transport, and the transfer of a large amount of Na^+ and Cl^- ions through the IEM resulted in a slow transfer of H^+ and OH^- ions. This was because of the maximum availability of initial salt concentration in FC when compared with the water dissociated ions. As the operation time passed, the dissociation of large amounts of water molecules resulted in the large accumulation of H^+ and OH^-. It should be noted that once all the Na^+ and Cl^- ions were transported from the FC, the accumulated H^+ and OH^- were also transported very efficiently resulting in the higher WDE after the first half performance time. This also explained the reason for the observed higher T. No. of ions with time during the first half part of the performance and a decrease in its value during the later stages of performance for the same membrane [18].

Ion transport number indicates the contribution of ions towards acid-base production, depending upon its electrical mobility under electric current. Fig. 10 represents the T. No. properties of both sodium and chloride ions for RPSu-Pt and PSDVB systems. It was from the figure that the T. No. of both Na^+ ion and Cl^- ions decreased with increase in time for both the systems. This was because NaCl concentration that was available for migration started to decrease with increase in time as discussed above. However, the performance was running steadily due to the current carried by the dissociated water products of H^+ and OH^- ions. In both IEM systems the chloride ion T. No. was observed to be greater than the sodium ion T. No. as reported in literature. The initially observed higher values of T. No. of sodium (0.17) and chloride (0.69) ions decreased to 0.04 and 0.1 respectively for RPSu-Pt system. Whereas, in the case of PSDVB based system, the T. No. of sodium and chloride ions decreased from their initial values of 0.4 and 0.5 to 0.37 and 0.42 respectively in brine desalination performance.
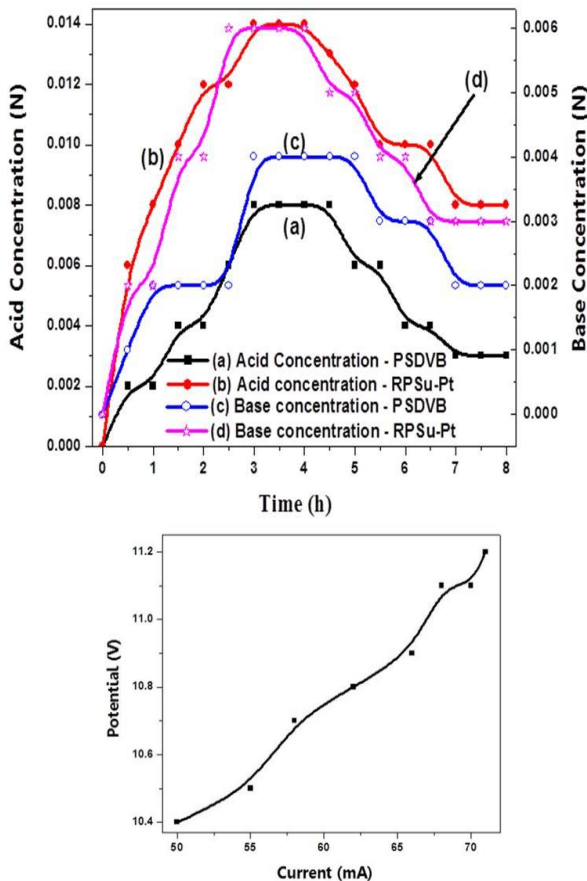

Fig. 9: I-V curves and acid-base yield with time

From Fig. 9, the current and voltage were observed to be directly proportional to each other thereby proving the water splitting at the BPM junction. The maximum potential observed was 11.2 V and 22.5 V and the maximum current observed was 71 mA and 89 mA for RPSu-Pt and PSDVB systems respectively. The observed lower voltage for RPSu-Pt system could be explained theoretically using protonation and de-protonation reactions model and the hydrophilicity change in the interface. The presence of polar interactions between the intermediate Pt and the water molecules speeds up the water
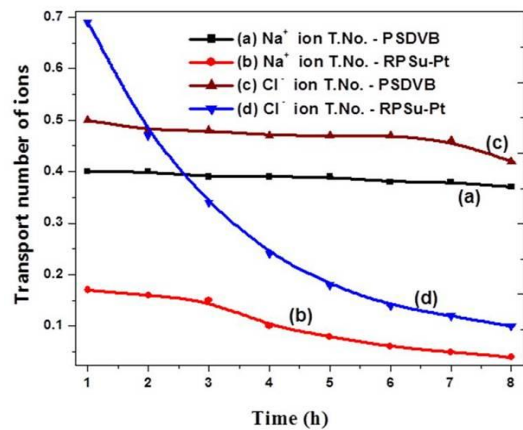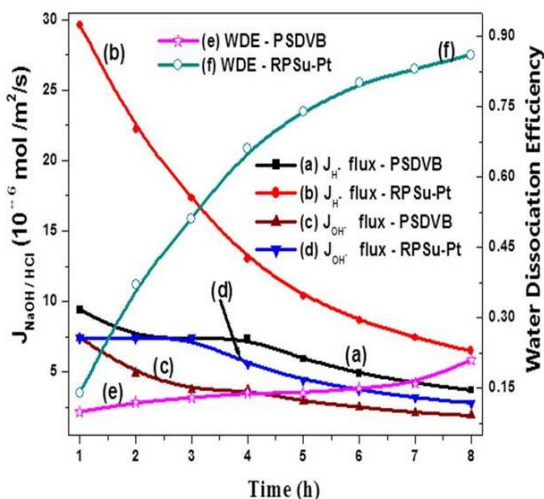
Fig. 10: Change in T. No. of ions, WDE, acidic and basic water dissociation fluxes with time

Based on feed concentration, membrane capacity and pH variation in AC and BC during the stack performance, the occurrence of water dissociation at BPM interface was confirmed. From Fig. 10, it was clear that WDE increased with increase in time. The reason for this variation of WDE with time is the same as discussed for T. No. of ions. A higher WDE of 0.86 was obtained for RPSu-Pt and it was 0.21 for PSDVB IEM system. The higher T. No. and steady increase in WDE with time observed for RPSu-Pt IEM system was due to (i) the increase in electric field, (ii) the pre-polarization of water molecules at the membrane-solution interface and (iii) the presence of a catalytic Pt intermediate in between the two monopolar layers of BPM. It was also noted from Fig. 10 that in both cases (acidic or basic), the water dissociation fluxes decreased with time. The main reason for the decrease in acid and base fluxes was due to (i) the depletion of Na^+ in anode compartment and Cl^- ion in cathode compartment and (ii) the availability of NaCl in FC for the conversion into the acid and base. The highest acidic and basic flux observed in the present study was 9.4×10^{-6} mol m^{-2} s^{-1} and 7.4×10^{-6} mol m^{-2} s^{-1} for PSDVB and 29.6×10^{-6} mol m^{-2} s^{-1} and 7.41×10^{-6} mol m^{-2} s^{-1} for RPSu-Pt systems respectively. According to Ren et al [19] the reduction in the ionic transport rate during later stages of the performance was often correlated with an increased membrane resistance due to the presence of a mixture of organic matter and inorganic salts. As a consequence, during performance of brine desalination, a slight membrane fouling was observed for both RPSu-Pt and PSDVB IEM systems.

(iv) Determination of process efficiency parameters and I-

V measurement

For any system, higher CE with lower energy consumption is one of the factors which determine the feasibility of electrochemical process towards higher process efficiency. It is clear from Fig. 11 that CE of BPMED stack decreased with operation time for both systems. This can be explained by invoking the concept of ion leakage through IEM as discussed in T. No. of ions. CE was observed to decrease with time from 38 % for PSDVB system and from 68.6 % for RPSu-Pt system. On the other hand, the energy consumption increased with time as shown in Fig. 11. The increase in the energy consumption was mainly attributed to the fact that a large part of the total electrical energy was consumed to overcome the electrical resistance. The decline in the applied voltage at the start of the BPMED procedure was due to either the increase in

conductivity of HCl/NaOH solution in AC/BC or due to the exhaustion of NaCl in the feed solution. The increase in resistance of FC, resulted from the exhaustion of NaCl in the solution, was offset by the decrease in electrical resistance of AC and BC caused by the increase in HCl and NaOH concentrations as a consequence of transfer of Cl^- and Na^+ ions from the feed solution. Since the transformation of NaCl into acid and base solution was fully realized, the electrical resistance of feed solution increased, resulting in a sharp increase in the voltage drop. Thus, the energy consumption was observed to increase with time and reached a maximum of 6.2 Wh for PSDVB and 6.24 Wh for RPSu-Pt systems.

The current variation was observed to increase with time for both RPSu-Pt and PSDVB systems as shown in Fig. 11 due to the production of OH^-/H^+ by water dissociation. In FC, the decrease in salt concentration due to continuous ion transport resulted in higher resistance. The higher resistance observed initially in AC and BC because of lower concentrations of acid and alkali decreased due to increase in acid and base concentration with increase in time. The net effect of this was the overall decrease in stack resistance with time. The difference in stack resistance and concentration polarization observed between two systems inferred a lower current of 70 mA for RPSu-Pt when compared to 89 mA for PSDVB system. In case of voltage versus time curve, a line parallel to X-axis indicated that both PSDVB and RPSu-Pt systems were chemically stable as described by Xue et al [20]. The purity of acid and alkali increased with increase in voltage to some extent, after which further increase in voltage caused heating of stack which resulted in the deterioration of membrane properties.
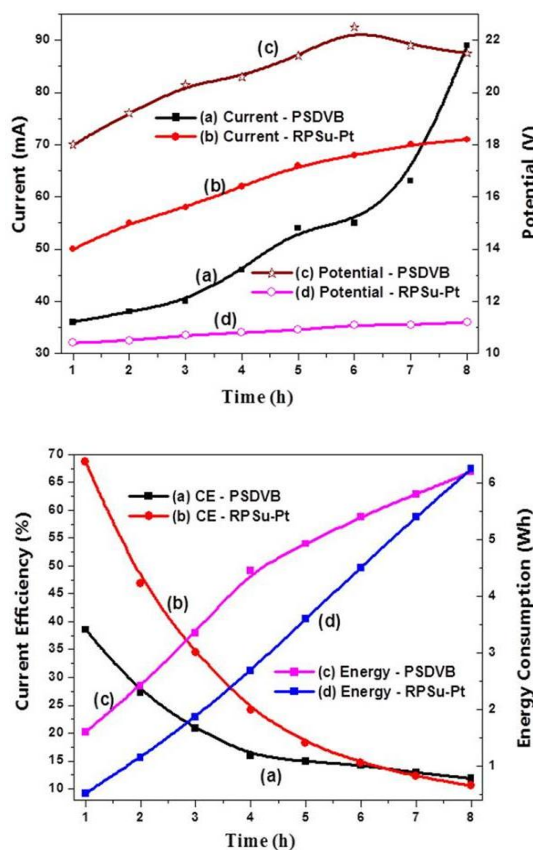

Fig. 11. *Change in current, potential, CE and energy consumption with time*

(v) Determination of Electrical conductivity, Salinity and

Sodium-Chloride ion Concentration

To evaluate the purity of the generated acid and base and to confirm the BPM's capacity to dissociate water, certain important parameters such as electrical conductivity, salinity, sodium ion and chloride ion concentrations were analyzed. Table 4 represents the initial and final values of electrical conductivity, salinity and sodium-chloride ion concentrations of 100 mL FC solution for both RPSu-Pt and PSDVB systems. Though the removal of NaCl ions from the FC was confirmed by its electrical conductivity measurements; the effectiveness of this process was confirmed by its salinity measurements. The observance of lower salinity and lower electrical conductivity than their initial values was mainly because of the migration of the salt ions from the FC towards the neighboring compartments. Thus, this result suggested that the water obtained after the BPMED desalination process was of better quality than the initial sample. The final FC solution showed lower sodium and chloride ion concentrations than their initial salt sample solution for both the systems. This once again, confirmed the migration of ions under the electric field from FC to the neighboring compartments. The higher difference between the initial and final values indicated the process effectiveness in removal of NaCl and higher acid-base production.

Table 4: Electrical conductivity, salinity and sodium-chloride ion concentration values for RPSu-Pt and PSDVB systems

Parameters		RPSu-Pt system	PSDVB system
Electrical conductivity	Initial	17.17	17.17
(mS/cm)	Final	6.92	12.02
Salinity	Initial	11.5	11.5
(%)	Final	4.3	7.9
Chloride ion concentration	Initial	10.3	10.3
(mg/100 mL)	Final	6.15	8.6
Sodium ion concentration	Initial	9	9
(ppm)	Final	4.1	8

IV. CONCLUSION

Resin-glass fiber reinforced and functionalized PSu IEMs were prepared and characterized using FTIR, TGA, SEM and contact angle measurements. The chemical stability of the prepared IEMs was evaluated by means of ionic conductivity, water absorption and IEC. The BPM efficiency of RPSu-Pt and PSDVB based systems were evaluated using pH, conductivity and concentration measurements. Brine desalination performance was analyzed for both RPSu-Pt and PSDVB based systems and compared. Based on the results obtained for current efficiency (68.6 % for RPSu-Pt and 38 % for PSDVB), lowest energy consumption (0.5 Wh for RPSu-Pt and 1.6 Wh for PSDVB), acid-base production (0.014 N acid & 0.006 N base for RPSu-Pt and 0.008 N acid & 0.004 N base for PSDVB) and WDE (0.86 for RPSu-Pt and 0.21 for PSDVB), it was concluded that RPSu-Pt based IEM system showed a better performance than that of the commercial PSDVB based IEM system.

References

[1] H.K. Lonsdale, "The growth of Membrane Technology," Journal of Membrane Science, vol. 10, 1982, pp. 81.

[2] V.V. Volkov, B.V. Mchedlishvili, V.I. Roldugin, S.S. Ivanchev, and A.B. Yaroslavtsev, "Membranes and Nanotechnologies," Nanotechnologies in Russia, vol. 3, 2008, pp. 656.

[3] O. Kuroda, S. Takahashi, S. Kubota, K. Kikuchi, Y. Eguchi, Y. Ikenaga, N. Sohma, K. Nishinoiri, S. Wakamatsu, and S. Itoh, "An electrodialysis sea water desalination system powered by photovoltaic cells," Desalination, vol. 67, 1987, pp. 33.

[4] G. Pourcelly, and C. Gavach, "Electrodialysis water splitting-application of electrodialysis with bipolar membranes," In: Kemperman, AJB (ed.), Handbook on Bipolar Membrane Technology, Twente University Press, Enschede, 2000.

[5] S. S. Ivanchev, "Fluorinated Proton-Conduction Nafion- Type Membranes, the Past and the Future," Russian Journal of Applied Chemistry, vol. 81, 2008, pp. 529.

[6] K. Venugopal, and S. Dharmalingam, "Fundamental studies on a new series of SPSEBS-PVA-QPSEBS bipolar membrane: membrane preparation and characterization," Journal of Applied Polymer Science, vol. 127, 2008, pp. 4983.

[7] K. Venugopal, and S. Dharmalingam, "Evaluation of synthetic salt water desalination by using a functionalized polysulfone based bipolar membrane electrodialysis cell," Desalination, vol. 344, 2014, pp. 189.

[8] K. Venugopal, and S. Dharmalingam, "Investigation on the application of polysulfone based bipolar membrane for desalination of water," Desalination and water treatment, vol. 54, 2015, pp. 285.

[9] B. Bauer, F.J. Gerner, and H. Strathmann, "Development of bipolar membranes," Desalination, vol. 68, 1988, pp. 279.

[10] O. Kedem, and A. Warshawsky, "A supported, mechanically stable bipolar membrane for electrodialysis," Patent to Yeda Research and development company, Ltd., Israel, EP 0,504,904 A2, 1992.

[11] K. Venugopal, and S. Dharmalingam, "Desalination efficiency of a novel bipolar membrane based on functionalized polysulfone," Desalination, vol. 296, 2012, pp. 37.

[12] M. Kumar, and V.K. Shahi, "Heterogeneous–homogeneous composite bipolar membrane for the conversion of salt of homologous carboxylates into their corresponding acids and bases," Journal of Membrane Science, vol. 349, 2010, pp. 130.

[13] C.R. Dias, and M.N. de Pinho, "Water structure and selective permeation of cellulose based membranes," Journal of Molecular Liquids, vol. 80, 1999, pp. 117.

[14] R. Guan, H. Zou, D. Lu, C. Gong, and Y. Liu, "Polyether sulfone sulfonated by chlorosulfonic acid and its membrane characteristics," European Polymer Journal, vol. 41, 2005, pp. 1554.

[15] S. Sachdeva, R.P. Ram, J.K. Singh, and A. Kumar, "Synthesis of anion exchange polystyrene membranes for the electrolysis of sodium chloride," AIChE Journal, vol. 54, 2008, pp. 940.

[16] X. Zhu, Y. Liang, H. Pan, X. Jian, and Y. Zhang, "Synthesis and properties of novel H-bonded composite membranes from sulfonated poly (phthalazinone ether)s for PEMFC," Journal of Membrane Science, vol. 312, 2008, pp. 59.

[17] A. Tanioka, K. shimizu, T. Hosono, R. Eto, and T. Osaki, "Effect of interfacial state in bipolar membrane on rectification and water splitting." Colloids and Surfaces A: Physicochemical and engineering aspects, vol. 159, 1999, pp. 395.

[18] J. Shen, J. Huang, L. Liu, W. Ye, J. Lin, and B.V. Bruggen, "The use of BMED for glyphosate recovery from glyphosate neutralization liquor in view of zero discharge." Journal of Hazardous Materials, vol. 260, 2013, pp. 660.

[19] H. Ren, Q. Wang, X. Zhang, R. Kang, S. Shi, and W. Cong, "Membrane fouling caused by aminoacid and calcium during bipolar membrane electrodialysis." Journal of chemical technology and biotechnology, vol. 83, 2008, pp. 1551.

[20] Y.H. Xue, R.Q. Fu, Y.X. Fu and T.W. Xu, "Fundamental studies on the intermediate layer of a bipolar membrane V. Effect of silver halide and its dope in gelatin on water dissociation at the interface of a bipolar membrane," Journal of Colloid and Interface Science, vol. 298, 2006, pp. 313.